Conductance quantization and transport gaps in disordered graphene nanoribbons

E. R. Mucciolo,[1] A. H. Castro Neto,[2] and C. H. Lewenkopf[3,4]
[1]*Department of Physics, University of Central Florida, P.O. Box 162385, Orlando, Florida 32816, USA*
[2]*Department of Physics, Boston University, 590 Commonwealth Avenue, Boston, Massachusetts 02215, USA*
[3]*Departamento de Física Teórica, Universidade do Estado do Rio de Janeiro, 20550-900 Rio de Janeiro, Brazil*
[4]*Laboratório Nacional de Luz Síncrotron, Caixa Postal 6192, 13084-971 Campinas, São Paulo, Brazil*
(Received 15 December 2008; published 3 February 2009)

We study numerically the effects of edge and bulk disorder on the conductance of graphene nanoribbons. We compute the conductance suppression due to Anderson localization induced by edge scattering and find that even for weak edge roughness, conductance steps are suppressed and transport gaps are induced. These gaps are approximately inversely proportional to the nanoribbon width. On/off conductance ratios grow exponentially with the nanoribbon length. Our results impose severe limitations to the use of graphene in ballistic nanowires.

DOI: 10.1103/PhysRevB.79.075407 PACS number(s): 73.23.−b, 73.50.−h, 81.05.Uw

I. INTRODUCTION

Measurements of electronic transport in graphene triggered an intense effort to understand the physical properties of this material.[1,2] Both fundamental and applied aspects are currently being investigated by a large number of groups around the world. As the quality of the samples improves and other synthesis techniques are developed, the material changes from a regime where bulk disorder is the dominant electron-scattering mechanism at low temperatures to a ballistic one, where boundary conditions, crystal alignment, and edge defects play a dominant role in setting the transport properties. This regime is now experimentally accessible in ultranarrow ribbons, which are promising for developing high-frequency low-noise low-power field-effect transistors.

Motivated by recent experiments[3–5] and theoretical studies,[6–14] in this paper we explore how edge roughness affects conductance in long nanoribbons with realistic widths from several nanometers to tens of nanometers. Through numerical simulations we show that even very weak edge disorder has a marked effect in the conductance of these nanoribbons. Moderate amounts of edge roughness can substantially suppress the linear conductance near the charge neutrality point and induce a transport gap when the nanoribbon is long and the number of propagating channels is small. This effect is a manifestation of quasi-one-dimensional Anderson localization. We compute transport gaps, localization lengths, and on/off ratios and explore the combined effect of edge and bulk disorders. We also comment on the effect of inelastic scattering and dephasing. For nanoribbons with very weak edge roughness, conductance steps appear at noninteger values of the conductance quantum e^2/h, irrespective of the lattice orientation. Our results indicate that producing quantum point contacts with current graphene nanoribbons will be extremely challenging and can only be achieved if either scattering at edges of the constriction is substantially suppressed or the edges themselves are defined with atomic precision. The paper is organized as follows. In Sec. II we describe the numerical method and present our results for the linear conductance of a graphene nanoribbon in the presence of edge disorder. In Sec. III we show the results of our computations when bulk disorder is added to the nanoribbons and in Sec. IV we discuss the effects of weak edge roughness on the conductance quantization steps of nearly ballistic nanoribbons. Conclusions and final comments are left to Sec. V.

II. TRANSPORT IN THE PRESENCE OF EDGE DISORDER

The simulations are based on the standard nearest-neighbor tight-binding model of a single-layer graphene.[2] The linear conductance is evaluated through the recursive Green's-function technique.[15] An infinite nanoribbon is broken into three parts (see Fig. 1): two (left and right) semi-infinite regions of width W modeling ideal contacts and a finite central region of length L where edge and bulk disorders are introduced.

For a nanoribbon with perfect edges and no bulk disorder,[16] the conductance near the neutrality point $E_F=0$ can be zero (for semiconductor armchair) or a multiple of the conductance quantum $2e^2/h$ (for metallic armchair and zigzag), depending on the availability of states. The first discontinuity in the conductance appears when the Fermi energy E_F matches the minimum of first electron or hole subband; other steps are reached as the minima of consecutive subbands are crossed.

In our simulations, edge defects are created by extracting lattice sites (carbon atoms) from both edges of the nanoribbon following a uniform probability distribution. It is assumed that atoms at the edges are always attached to two other carbon atoms and passivated by a neutral chemical ligand, such as hydrogen. The control parameters are the number of etching sweeps N_{sweep}, which is related to the roughness amplitude, and the etching probability per site in the kth sweep, p_k, which is related to the edge defect density. Unless otherwise specified, an averaging over ten realiza-

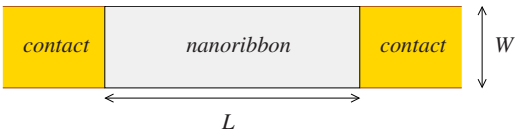

FIG. 1. (Color online) Schematic representation of the graphene nanoribbon setup used in the simulations.

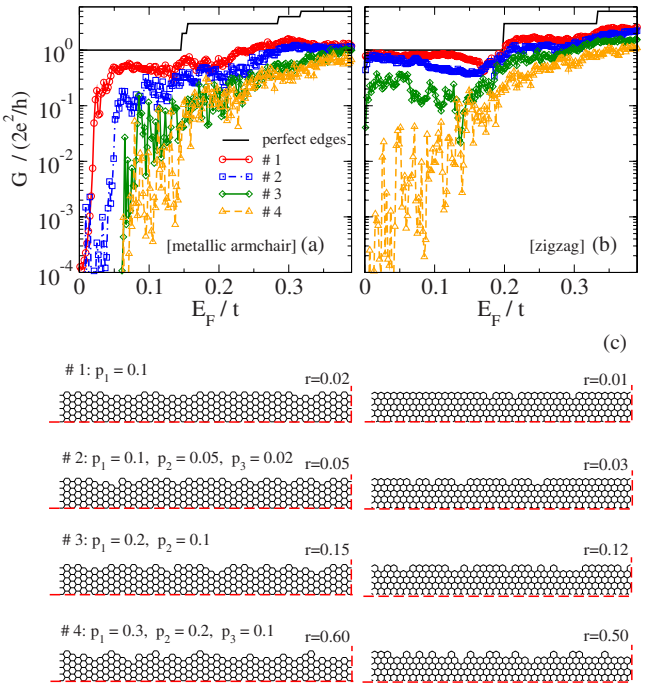

FIG. 2. (Color online) (a) and (b) Energy dependence of the average linear conductance of graphene nanoribbons with varying edge roughness. All nanoribbons have the same length (L =45 nm) and similar widths (W=4.4 nm for armchair and W =4.7 nm for zigzag). (c) Typical etching profiles used in (a) and (b) (only segments of the nanoribbon atomic structure are shown). Left: armchair and right: zigzag.

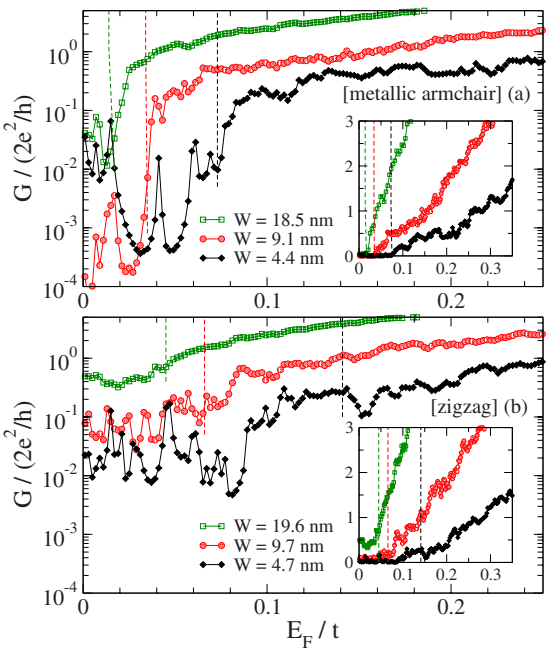

FIG. 3. (Color online) Average conductance of (a) metallic armchair (W=4.3 nm) and (b) zigzag (W=4.6 nm) nanoribbons as a function of the Fermi energy for three different widths when moderate roughness is present (zero temperature). The dashed lines indicate the conductance gap estimated by the change in the slope of the curves (see insets). A total of ten realizations of the edge roughness types 3 for armchair and 4 for zigzag were used for each curve presented.

tions of each disorder case analyzed was carried out to decrease sample-to-sample fluctuations and facilitate the visualization of the results.

In Figs. 2(a) and 2(b) we show the linear conductance of nanoribbons with metallic armchair and zigzag lattice orientations as a function of the Fermi energy for different values of N_{sweep} and $\{p_k\}$ at zero temperature. Also shown in Fig. 2(c) are the typical etching profiles for the four different cases. We have defined the roughness parameter $r=(W-\bar{W})P/a_0$, where $\bar{W}$ is the average ribbon width, $P=\Sigma_k p_k$, and a_0 is the lattice constant.[17] While a staircase of conductance steps is seen in the absence of edge roughness, the conductance rapidly degrades as the concentration and depth of the random etching increase. The conductance is strongly suppressed near the neutrality point even for relatively shallow etchings. Close to the neutrality point, a deep gap develops.

The formation of a transport gap in ultranarrow graphene nanoribbons is very much consistent with all experimental evidence available so far.[3,18,19] Several mechanisms have been proposed to account for this phenomenon, such as straightforward lateral confinement to many-body effects.[20,21] Some of these mechanisms require the existence of substantial edge disorder along the ribbon (enough, for instance, to form bottlenecks and quantum dots.[21])

The results presented in Figs. 2(b) and 2(c) show that the suppression of conductance can also occur at small values of r. Near the neutrality point, the number of propagating channels in the nanoribbon is very small and the system behaves as a quasi-one-dimensional wire. Edge defects act as randomly positioned short-range scatterers and induce strong backscattering, which in turn leads to Anderson localization if the nanoribbon is longer than the localization length. Note that even at room temperatures, we expect dephasing lengths in graphene to be exceedingly long.[22] Therefore, in practice, localization lengths can be shorter than both the nanoribbon length and the dephasing length.

Further evidence of this effect is provided in Figs. 3(a) and 3(b) where the conductance as a function of Fermi energy is shown for three different nanoribbon widths. At a fixed energy, for nanoribbons with increasing width, the localization becomes weaker and, consequently, the conductance suppression decreases. In order to make contact with experiments, we estimated transport gaps by determining the energy value at which the curves show an inflection point [see insets of Figs. 3(a) and 3(b)]. This inflection point corresponds to the crossing between two straight lines: an energy-independent conductance at low energies and a linear function at high energies. The results are shown in Fig. 4(a). For both lattice orientations, we find that the transport gap E_g scales approximately with the inverse of the nanoribbon width W and is only weakly dependent on the length L provided the latter is sufficiently long (not shown). Notice that the value obtained for A, the scaling prefactor, is in the same range of those found experimentally ($A \approx 0.2-0.6$ eV nm) (Refs. 18 and 19) even for moderate roughness. The gap is less pronounced for zigzag nanoribbons since for this orien-

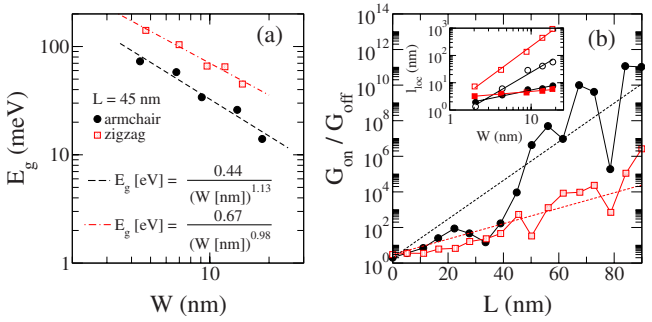

FIG. 4. (Color online) (a) Transport gap dependence on the nanoribbon width. The dashed and dashed-dotted lines are fittings to the data as explained in the main text. (b) On/off linear conductance ratio as a function of ribbon length. The solid lines are guides for the eyes and the dashed lines indicate fittings to exponential curves. Each data point corresponds to an average over 50 realizations of edge roughness. Inset: localization length as a function of ribbon width (circles are for armchair and squares are for zigzag). Solid (empty) symbols represent $E_F=0$ ($E_F=0.2t$). Lines are fittings of the functional form $\xi=AW^{\alpha}$ (see main text).

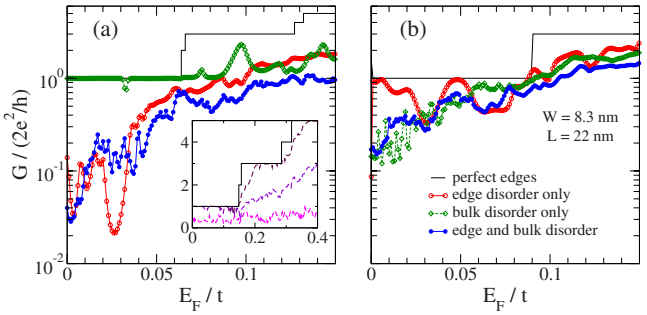

FIG. 5. (Color online) The effect of combined edge and bulk disorders on the average conductance of short graphene nanoribbons. (a) Armchair and (b) zigzag orientations (both with the same width $W=8.3$ nm and length $L=22$ nm). The edge disorder corresponds to the case 2 of Fig. 2(c); the bulk disorder has parameters $n_{\mathrm{imp}}=0.04$, $K_0=0.5$, and $\xi=2a_0$. Inset: average linear conductance of armchair nanoribbons with bulk disorder and perfect edges at zero temperature ($L=22$ nm, $W=4.4$ nm and five realizations per curve). The dashed lines correspond to correlation lengths $\xi/a_0=10$, 3, and 1 from top to bottom ($n_{\mathrm{imp}}=0.02$ and $K_0=1$ in all three cases).

tation most of the current at low doping is carried through bulk states[5] which are less sensitive to edge defects. Nevertheless, once the etching goes deeper than one lattice spacing, a clear gap develops for zigzag orientations as well.

In Fig. 4(b) we plotted the ratio between the on and off linear conductances as a function of the nanoribbon length. The off conductance G_{off} was obtained at $E_F=0$ while G_{on} was defined as the conductance at the Fermi energy where a transition from the first to the second step occurs in the clean nanoribbon. The curves indicate an approximate exponential growth in the on/off ratio, consistent with the Anderson localization picture. Since conductance is broadly distributed in the localized regime, the on/off ratio develops very large fluctuations when the nanoribbon is long. In the inset we show the localization length l_{loc} extracted by fitting to the data an expression of the form $G(L)=G(0)e^{-L/l_{\mathrm{loc}}}$. We note that the localization length grows with increasing ribbon width and energy. Fittings to the form $l_{\mathrm{loc}}=AW^{\alpha}$ yield $\alpha=0.21-0.61$ at $E_F=0$ and $\alpha=1.8-2.2$ at $E_F=0.2t$, with the prefactor in the range $A=0.04-7.3$ for l_{loc} and W in lattice units. Thus, l_{loc} can be comparable to W.

III. BULK DISORDER

In order to investigate the effects of bulk disorder, we added an on-site correlated Gaussian disordered potential $U_{\mathrm{imp}}(\mathbf{r})$ to the nanoribbon.[23–25] The latter is constructed by distributing along the nanoribbon N_{imp} Gaussian scatterers of width ξ with random amplitudes $\{U_n\}$ drawn from a uniform distribution $[-\delta U, \delta U]$. The intensity of the disorder is characterized by the dimensionless parameter K_0, which is defined through the correlation function

$$\langle U_{\mathrm{imp}}(\mathbf{r}_i)U_{\mathrm{imp}}(\mathbf{r}_j)\rangle = K_0\frac{\hbar v}{2\pi\xi^2}e^{-|\mathbf{r}_i-\mathbf{r}_j|^2/2\xi^2}. \quad (1)$$

In the dilute limit, when N_{imp} is much smaller than the total number of sites in the nanoribbon, one can show that[24] $K_0 \approx 40.5 n_{\mathrm{imp}}(\delta U/t)^2(\xi/a_0)^4$, where n_{imp} is the scatterer density per lattice site. For large graphene sheets at high doping, far from the neutrality point, it is possible to relate this parameter to the transport mean-free path using the Born approximation[25] $\ell_{\mathrm{tr}}=2\lambda_F/\pi K_0$, where λ_F is the Fermi wavelength in the graphene sheet, with $\lambda_F \ll \ell_{\mathrm{tr}}$.

The difference between armchair and zigzag states near the neutrality point also explains the effect of bulk disorder in nanoribbons with rough edges (Fig. 5). For the metallic armchair orientation the low-lying states are concentrated at the edges and are quite sensitive to edge roughness.[6] In this case, moderate bulk disorder has a small effect on the transport gap. For zigzag orientations, the situation is the opposite as bulk disorder disrupts the current-carrying states and suppresses conductance in this case. However, for both orientations, bulk disorder only leads to strong localization when $\xi \lesssim a_0$ (short-range disorder).

IV. CONDUCTANCE QUANTIZATION

While it is clear that moderate edge disorder leads to substantial suppression of the conductance of nanoribbons, what happens when the etching is nearly perfect and only very few and shallow defects are present? How does weak edge roughness affect conductance quantization in comparison to bulk disorder? Answers to these questions are provided in Fig. 6 and in the inset of Fig. 5(a). The main effect of very weak edge disorder is to lower the conductance steps *without* changing their positions in energy. Some fluctuations occur near the transition regions between steps because of the sensitivity of the evanescent modes to variations in nanoribbon width, but these fluctuations are washed out at finite temperatures. However, thermal fluctuations, even at room temperature, do not change the wider steps, as can be seen in the insets of Fig. 6, as long as the nanoribbon is sufficiently narrow.

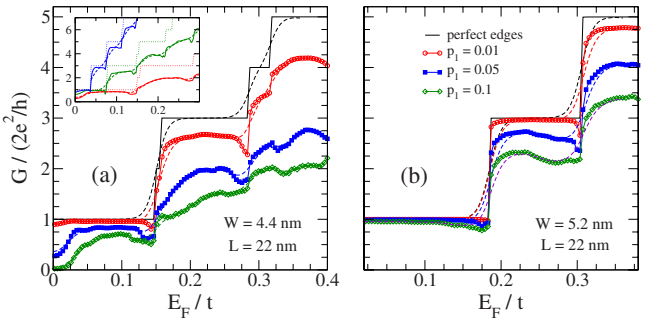

FIG. 6. (Color online) Suppression of conductance quantization steps due to weak edge disorder. (a) Armchair and (b) zigzag orientations. A total of 100 realizations were used in each case. Solid (dashed) lines indicate zero (room) temperature in the contacts. Inset: average conductance versus energy for a metallic armchair nanoribbon with $L=22$ nm, no bulk disorder, $p_1=0.05$ (ten realizations), and increasing widths $W=4.4$, 9.1, and 18.5 nm; solid (dashed) lines represent zero (room) temperature, while dotted lines describe the perfect edge case at zero temperature.

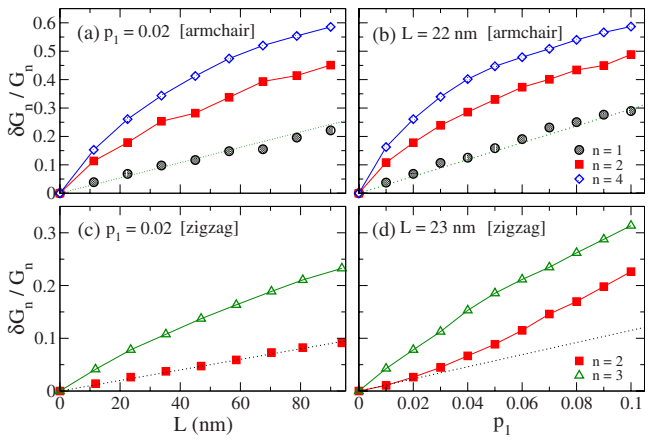

FIG. 7. (Color online) Relative suppression of the nth conductance step as a function of (a) and (c) nanoribbon length and (b) and (d) defect concentration for metallic armchair ($W=4.4$ nm) and zigzag ($W=5.2$ nm) orientations. Each data set corresponds to an average over 100 realizations. The index n indicates the order of the conductance step and the solid lines are guides for the eyes. The dotted lines are explained in the main text.

Bulk disorder, on the other hand, has a quite distinct effect on the conductance quantization. In the inset of Fig. 5(a) we show how bulk disorder affects the conductance steps of a metallic armchair nanoribbon. As the disorder range widens, the steps are smeared without shifting the conductance value. This result can be understood in the following way. When only weak edge disorder is present, the width of the nanoribbon is hardly unaltered and propagating channels in the nanoribbon open up at the same energies as in the case of perfect edges. Yet, backscattering due to randomly positioned edge defects, albeit weak, reduces the overall conductance and shifts the steps downward. Long-range bulk disorder, on the other hand, creates potential inhomogeneities which lead to the appearance of electron and hole puddles when the Fermi energy lies close to the Dirac point.[23] Transmission through these puddles creates mode mixing, which in turn smears the conductance steps.

A simple model can be used to describe the suppression of the conductance steps. For the first step, let us assume that carriers propagate in one dimension through a sequence of randomly positioned but identical barriers. When the barrier reflectance is very small, $R \ll 1$, it is straightforward to show that, in the short-wave limit ($\lambda \ll L$), the conductance in the first step goes as $G_1 \approx (2e^2/h)[1-NR]$, where N is the number of barriers, which can be directly related to the defect probability or density as follows: $N=(L/a_0)p_1$. For higher steps, more than one propagating mode is present and the system becomes quasi-one dimensional. In the absence of mode mixing, the conductance of the nth step behaves as $G_n \approx n(2e^2/h)[1-NR]$. However, mode mixing is unavoidable for $n>1$ and one expects strong deviations from this simple scaling behavior

The suppression of the conductance step as a function of nanoribbon length and edge defect concentration is presented in Fig. 7. For the first step of the armchair orientation the simple one-dimensional scattering model works quite well. Both dashed lines in Figs. 7(a) and 7(b) correspond to $R=0.035$. The linear scaling ceases to apply for higher steps, with a sublinear dependence indicating substantial mode mixing. For zigzag orientations, the suppression of the first conductance step was too small to be shown on the same plot. Figures 7(c) and 7(d) show that the simple scaling behavior no longer applies already when $n=2$ ($R=0.013$ was used in this case).

V. CONCLUSIONS

Our results indicate that creating graphene quantum point contacts will depend fundamentally on atomic-scale engineering.[26] In searching for ways to improve the nanoribbon conductance in the presence of edge roughness, we found that, due to the Klein tunneling effect, side gates are not effective in reducing edge scattering (i.e., electrostatic potentials do not confine Dirac fermions). At moderate roughness, Anderson localization develops and transport gaps appear. There is a quantitative agreement between the gaps that we find numerically when extrapolating our results to wider nanoribbons and the available experimental data, although we expect that other mechanisms, such as spin gaps[20] and charging effects[21] (not taken into account in our calculations), will likely compete with localization. Electronic dephasing can be introduced in the calculation following a standard procedure.[27] Since, in practice, dephasing lengths exceed the nanoribbon width, we expect that the main effect of dephasing will be the appearance of an additional weakly energy-dependent suppression of the conductance as the nanoribbon will break into a series of independent quantum resistors. At this point, we would also like to note that we recently became aware of similar work by Evaldsson *et al.*[28]

ACKNOWLEDGMENTS

We thank I. Adagideli, H. Dai, D. Goldhaber-Gordon, M. Ishigami, Y.-M. Lin, I. Martin, and K. Todd for helpful

discussions. E.R.M. and A.H.C.N. thank the Aspen Center for Physics, where this work was completed. C.H.L. thanks FAPERJ and CNPq (Brazil) for partial financial support. A.H.C.N. acknowledges the partial support of the U. S. Department of Energy under Grant No. DE-FG02–08ER46512.

[1] A. K. Geim and K. S. Novoselov, Nature Mater. **6**, 183 (2007).
[2] A. H. Castro Neto, F. Guinea, N. M. R. Peres, K. S. Novoselov, and A. K. Geim, Rev. Mod. Phys. (to be published).
[3] X. Wang, Y. Ouyang, X. Li, H. Wang, J. Guo, and H. Dai, Phys. Rev. Lett. **100**, 206803 (2008).
[4] Y.-M. Lin, V. Perebeinos, Z. Chen, and P. Avouris, Phys. Rev. B **78**, 161409(R) (2008).
[5] K. Todd, H.-T. Chou, S. Amash, and D. Goldhaber-Gordon, Nano Lett. **9**, 416 (2009).
[6] D. A. Areshkin, D. Gunlycke, and C. T. White, Nano Lett. **7**, 204 (2007).
[7] Q. Yan, B. Huang, J. Yu, F. Zheng, J. Zang, J. Wu, B.-L. Gu, F. Liu, and W. Duan, Nano Lett. **7**, 1469 (2007).
[8] T. C. Li and S.-P. Lu, Phys. Rev. B **77**, 085408 (2008).
[9] I. Martin and Ya. M. Blanter, arXiv:0705.0532 (unpublished).
[10] D. Querlioz, Y. Apertet, A. Valentin, K. Huet, A. Bournel, S. Galdin-Retalleau, and P. Dollfus, Appl. Phys. Lett. **92**, 042108 (2008).
[11] Y. Takane and K. Wakabayashi, J. Phys. Soc. Jpn. **77**, 054702 (2008).
[12] L. Yang, C.-H. Park, Y.-W. Son, M. L. Cohen, and S. G. Louie, Phys. Rev. Lett. **99**, 186801 (2007).
[13] F. Munoz-Rojas, D. Jacob, J. Fernandez-Rossier, and J. J. Palacios, Phys. Rev. B **74**, 195417 (2006).
[14] J. P. Robinson and H. Schomerus, Phys. Rev. B **76**, 115430 (2007).
[15] H. U. Baranger, D. P. DiVincenzo, R. A. Jalabert, and A. D. Stone, Phys. Rev. B **44**, 10637 (1991).
[16] N. M. R. Peres, A. H. Castro Neto, and F. Guinea, Phys. Rev. B **73**, 195411 (2006); J. Tworzydlo, B. Trauzettel, M. Titov, A. Rycerz, and C. W. J. Beenakker, Phys. Rev. Lett. **96**, 246802 (2006).
[17] This is a sensible definition only when $P \ll 1$.
[18] M. Y. Han, B. Özyilmaz, Y. Zhang, and P. Kim, Phys. Rev. Lett. **98**, 206805 (2007).
[19] Z. Chen, Y.-M. Lin, M. J. Rooks, and P. Avouris, Physica E **40**, 228 (2007).
[20] Y.-W. Son, M. L. Cohen, and S. G. Louie, Phys. Rev. Lett. **97**, 216803 (2006).
[21] F. Sols, F. Guinea, and A. H. Castro Neto, Phys. Rev. Lett. **99**, 166803 (2007).
[22] L. G. Cançado, R. Beams, and L. Novotny, arXiv:0802.3709 (unpublished).
[23] C. H. Lewenkopf, E. R. Mucciolo, and A. H. Castro Neto, Phys. Rev. B **77**, 081410(R) (2008).
[24] A. Rycerz, J. Tworzydło, and C. W. J. Beenakker, EPL **79**, 57003 (2007).
[25] N. H. Shon and T. Ando, J. Phys. Soc. Jpn. **67**, 2421 (1998).
[26] L. Tapasztó, G. Dobrik, P. Lambin, and L. P. Biro, Nat. Nanotechnol. **3**, 397 (2008).
[27] J. L. D'Amato and H. M. Pastawski, Phys. Rev. B **41**, 7411 (1990).
[28] M. Evaldsson, I. V. Zozoulenko, H. Xu, and T. Heinzel, Phys. Rev. B **78**, 161407(R) (2008).